ECCOMAS Congress 2016
VII European Congress on Computational Methods in Applied Sciences and Engineering
M. Papadrakakis, V. Papadopoulos, G. Stefanou, V. Plevris (eds.)
Crete Island, Greece, 5–10 June 2016

MODAL PROPERTIES AND SEISMIC RESPONSE OF EXISTING BUILDING RETROFITTED BY EXTERNAL BRACINGS WITH VISCOUS DAMPERS

Laura Gioiella[1], Enrico Tubaldi[2], Fabrizio Gara[1] and Andrea Dall'Asta[3]

[1] DICEA – Università Politecnica delle Marche
via Brecce Bianche, 60121 Ancona, Italy
l.gioiella,f.gara@univpm.it

[2] Department of Civil Engineering – Imperial College
Skempton Building, South Kensington Campus, Imperial College London, SW7 2AZ, UK
etubaldi@ic.ac.uk

[3] Scuola di Architettura e Design – Università di Camerino
Viale delle Rimembranze, 63100 Ascoli Piceno, Italy
andrea.dallasta@unicam.it

Keywords: Passive Seismic Protection, Linear Viscous Dampers, External Seismic Retrofit, Dissipative Towers.

Abstract. *This paper deals with the seismic protection of existing buildings using external viscous damper systems to increase the energy dissipation capacity. Dampers and bracings can be arranged in very different configurations and the possible solutions can be grouped into different categories, depending on the specific kinematic behavior. The study analyzes a recent solution called "dissipative tower", which, for the dampers activation, exploits the rocking motion of a stiff steel truss hinged at the foundation level. A state space formulation of the dynamic problem is presented in general terms and some issues concerning the influence of the bracing properties on the behavior of a case study consisting of a building coupled with a dissipative tower are investigated. The results presented concern both the influence of the external dissipative bracings on the most important modal properties of the system, and the global effect on the seismic response, evaluated via the modal decomposition method. It is shown that the addition of the towers yields a regularization of the drift demand along the building height, but it can also induce significant changes in the distribution of internal actions in the existing frame. Moreover, the contribution of higher order modes can be important for the internal actions evaluation, while it is negligible for the displacement estimation. The results obtained by considering the coupled system are compared with the corresponding results obtained by considering two limit cases: the bare frame, and the frame equipped with an infinitely stiff dissipative tower.*

1 INTRODUCTION

Passive control systems have proven to be very efficient solutions for new constructions and for seismic retrofitting of existing structures [1-4]. Viscous dampers are traditionally installed within a building frame in either diagonal or chevron brace configurations connecting adjacent storeys and there are many studies concerning both the dynamic properties of the damped system and the methods for the design [*e.g.*, 5-10]. However, this type of damping system may present some disadvantages, particularly when employed for retrofitting existing buildings. Usually, the addition of dissipative diagonal in existing frames provides an increment of axial forces in the columns and this may lead to premature local failures [11]. Furthermore, there may be some feasibility limits on the strengthening of the existing foundations at the base of the bracing system. Also, the indirect costs related to the interruption of the building utilization during execution of the retrofit can be very demanding, in particular for strategic buildings, such as hospitals or schools.

These problems can be efficiently resolved by considering external damper configurations, i.e., by placing the dissipative bracings and the relevant foundations outside the building frame. External dampers and bracing components can be arranged in very different configurations and the possible solutions can be grouped into three main categories, characterized by substantially different kinematic behaviors, but all permitting the control of both the total amount of the dissipated energy and the frame deformation at the various storeys. A possible solution can be obtained by placing the dampers horizontally at the storey level, between the frame and an external stiff structure [12]. This way, the links are activated by the floor absolute displacements. A similar configuration can be obtained by placing the dampers between adjacent buildings, though this solution is efficient if the two buildings have strongly different dynamic properties [13-16]. An alternative solution can be obtained by coupling the frame with an external shear deformable bracing structure. The new and existing structures are connected at the storey level and the dissipative devices are activated by the relative displacements between adjacent floors, as in the more traditional case of bracings placed within the existing structure [3].

Recently, some applications have been developed by proposing a new configuration exploiting the rocking motion of a stiff brace hinged at the foundation level [17, 18]. In this configuration, known as "dissipative tower" (Figure 1) [19], the dampers are activated by the base rotation of the tower.

This work focuses on the coupling between an existing frame and a rocking dissipative configuration shown in Figure 1; the purpose is the investigation of the modal properties and the seismic response of the coupled system by means of a problem formulation presented in general terms. The dynamic behavior and seismic performance of the system is compared against that of two other limit cases, the first one being the bare building, the second the building coupled with an infinitely stiff dissipative tower.

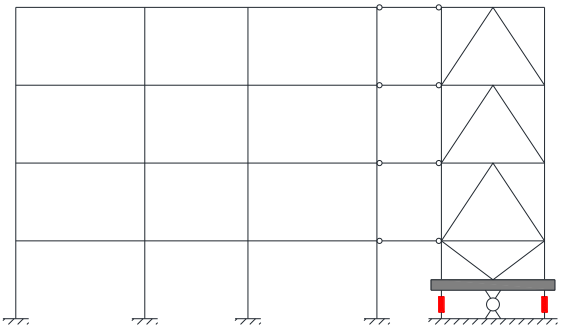

Figure 1: Dissipative Tower.

2 PROBLEM FORMULATION

In the first part of this section, the equation of motion and the state variables of the considered problem are presented by assuming that both the building and the external damping system exhibit a linear response. The limit case of stiff tower is also presented and the balance equations of the reduced single-degree-of-freedom (SDOF) system are obtained by introducing a constraint in the structure motion.

2.1 Equation of motion

The equations of motion for the system can be expressed as follows:

$$\mathbf{M}\,\ddot{\mathbf{u}}(t) + \mathbf{C}\,\dot{\mathbf{u}}(t) + \mathbf{K}\mathbf{u}(t) = \mathbf{M}\mathbf{p}\,a_g(t) \tag{1}$$

where $\mathbf{u}(t) \in R^l$, is the vector of nodal displacements, the dot (·) denotes time-derivative; $\mathbf{p} \in R^l$ is the load distribution vector, l denotes the total number of degrees-of-freedom, and $a_g(t)$ is the external scalar loading function describing the seismic base acceleration. The time invariant matrices $\mathbf{M}$, $\mathbf{K}$, $\mathbf{C}$ describe the mass, stiffness and damping operators $R^l \to R^l$; they result from the sum of the contribution due to the existing frame and the one coming from the external dissipative bracing system. The damping contribution of the frame and of the dissipative system are denoted respectively as $\mathbf{C}_F$ and $\mathbf{C}_D$. Generally, the external bracing system notably influences the stiffness and damping operators while it contributes only marginally to the mass operator. The displacement vector $\mathbf{u}(t)$ collects both the displacements required for the description of the frame response and the displacements involved in the bracing deformations.

In order to study the dynamic response of the system it is useful to separate the displacements associated with the masses, and thus involving inertial forces, from the displacements describing the internal degrees of freedom, related to stiffness and damping forces only. Accordingly, the total displacement vector $\mathbf{u}(t)$ can be split into the active components collected in the vector $\mathbf{x}(t) \in R^m$ and the other components $\mathbf{y}(t) \in R^n$ ($l = m + n$). The matrices describing the linear operators and the distribution vector can be consequently partitioned as follows

$$\begin{vmatrix} \mathbf{M}_{xx} & 0 \\ 0 & 0 \end{vmatrix} \begin{vmatrix} \ddot{\mathbf{x}} \\ \ddot{\mathbf{y}} \end{vmatrix} + \begin{vmatrix} \mathbf{C}_{xx} & \mathbf{C}_{xy} \\ \mathbf{C}_{yx} & \mathbf{C}_{yy} \end{vmatrix} \begin{vmatrix} \dot{\mathbf{x}} \\ \dot{\mathbf{y}} \end{vmatrix} + \begin{vmatrix} \mathbf{K}_{xx} & \mathbf{K}_{xy} \\ \mathbf{K}_{yx} & \mathbf{K}_{yy} \end{vmatrix} \begin{vmatrix} \mathbf{x} \\ \mathbf{y} \end{vmatrix} = \begin{vmatrix} \mathbf{M}_{xx} & 0 \\ 0 & 0 \end{vmatrix} \begin{vmatrix} \mathbf{p}_x \\ 0 \end{vmatrix} a_g \tag{2}$$

As usual, only the masses related to the horizontal floor displacements are considered in order to reduce the dimension of the dynamic problem and to simplify the interpretation of the results.

The distribution of the damping in the structure and, in particular, the location of the concentrated dampers of the external bracings, leads to a non-classically damped system. For its solution it is convenient to formulate the problem by introducing the vector $\mathbf{v}(t) = \dot{\mathbf{x}}(t)$ and the state vector $\mathbf{z}(t)$ collecting the displacements and the velocities of the active displacements and the displacements of the internal nodes:

$$\mathbf{z}(t) = \begin{vmatrix} \mathbf{x}(t) \\ \mathbf{v}(t) \\ \mathbf{y}(t) \end{vmatrix} \tag{3}$$

Eqn. (1) can be reduced to a first-order state space form:

$$\dot{\mathbf{z}}(t) = \mathbf{A}\mathbf{z}(t) + \tilde{\mathbf{p}}\, a_g(t) \tag{4}$$

where:

$$\mathbf{A} = \begin{vmatrix} \mathbf{0} & \mathbf{I} & \mathbf{0} \\ -\mathbf{M}_{xx}^{-1}\left(\mathbf{K}_{xx} - \mathbf{C}_{xy}\mathbf{C}_{yy}^{-1}\mathbf{K}_{yx}\right) & -\mathbf{M}_{xx}^{-1}\left(\mathbf{C}_{xx} - \mathbf{C}_{xy}\mathbf{C}_{yy}^{-1}\mathbf{C}_{yx}\right) & -\mathbf{M}_{xx}^{-1}\left(\mathbf{K}_{xy} - \mathbf{C}_{xy}\mathbf{C}_{yy}^{-1}\mathbf{K}_{yy}\right) \\ -\mathbf{C}_{yy}^{-1}\mathbf{K}_{yx} & -\mathbf{C}_{yy}^{-1}\mathbf{C}_{yx} & -\mathbf{C}_{yy}^{-1}\mathbf{K}_{yy} \end{vmatrix} \tag{5}$$

Vector $\tilde{\mathbf{p}}$ is defined as:

$$\tilde{\mathbf{p}} = \begin{vmatrix} 0 \\ \mathbf{M}_{xx}^{-1}\mathbf{p} \\ 0 \end{vmatrix} \tag{6}$$

2.2 Free vibrations and modal properties

The free vibration problem can be solved by assuming a solution of the form $\mathbf{z}(t) = \boldsymbol{\varphi} e^{\lambda t}$, where $\lambda, \boldsymbol{\varphi}$ are a eigenvalue-eigenvector pair of $\mathbf{A}$, such that:

$$\mathbf{A}\boldsymbol{\varphi} = \lambda\boldsymbol{\varphi} \tag{7}$$

Complex eigenvalue has the following form:

$$\lambda_i = -\xi_i\omega_{0i} + i\omega_{0i}\sqrt{1-\xi_i^2} \tag{8}$$

and contains information regarding both the damping ratio ξ_i and the corresponding undamped circular frequency ω_{0i} of the *i*-th mode. These information can be extrapolated as follows:

$$\begin{aligned} \omega_{0i} &= |\lambda_i| \\ \xi_i &= -\mathrm{Re}(\lambda_i)/|\lambda_i| \end{aligned} \tag{9}$$

Known the modal properties, the problem solution can be obtained as a linear combination of the single mode contributions. Let $\boldsymbol{\Lambda}$ be the diagonal matrix containing the complex eigenvalues and $\boldsymbol{\Phi} = |\boldsymbol{\varphi}_1, \boldsymbol{\varphi}_2, ..., \boldsymbol{\varphi}_{2m+n}|$ the complex eigenmatrix containing the eigenvectors, such that the orthogonality property $\boldsymbol{\Lambda} = \boldsymbol{\Phi}^{-1}\mathbf{A}\boldsymbol{\Phi}$ holds.

2.3 Seismic response via modal decomposition method

The motion can be obtained as a linear combination of modes:

$$\mathbf{z}(t) = \boldsymbol{\Phi}\mathbf{q}(t) \tag{10}$$

where $\mathbf{q}(t)$ is a vector collecting the modal coordinates. The orthogonality property leads to the diagonal problem:

$$\dot{\mathbf{q}}(t) = \boldsymbol{\Lambda}\mathbf{q}(t) + \boldsymbol{\gamma}\, a_g(t) \tag{11}$$

where $\gamma_i = \left[\boldsymbol{\Phi}^{-1}\tilde{\mathbf{p}}\right]_i$ is the *i*-th (complex-valued) modal participation factor.

Introducing the normalized complex modal response vector $\mathbf{s}(t)$ such that: $q_i(t) = \Gamma_i s_i(t)$, the problem can be written in a normalized form:

$$\dot{\mathbf{s}}(t) = \mathbf{\Lambda s}(t) + \mathbf{I}a_g(t) \tag{12}$$

Assuming that the system is initially at rest, the solution can be obtained by the Duhamel integral:

$$\mathbf{s}(t) = \int_0^t \mathbf{h}(t-\tau)a_g(\tau)d\tau \tag{13}$$

where the components $h_i(t) = e^{\lambda_i t}$ are the solutions related to an impulsive unitary input.

2.4 Generalized SDOF system approximation

The dissipative tower consists of an external bracings system that activates the dampers located at its base through its rocking motion. In the case of an infinitely stiff tower all the degrees of freedom of the system (active displacements of the frame and displacements involved in the bracing deformations) are governed by the base rotation φ. This means that the displacement vector $\mathbf{u}(t)$, shown in eqn. 1, can be expressed as

$$\mathbf{u}(t) = \mathbf{L}\varphi \tag{14}$$

in which **L** is a vector collecting the heights of the frame. The D'Alembert Principle for the problem at hand can be expressed by introducing a virtual velocity field $\hat{\eta} = \mathbf{L}\hat{\varphi}$, in which $\hat{\varphi}$ is an arbitrary base rotation. Eqn. 1 can be rewritten for any time instant *t* as

$$\mathbf{M}_b\ddot{\mathbf{u}}\cdot\hat{\eta} + \mathbf{C}_F\dot{\mathbf{u}}\cdot\hat{\eta} + \mathbf{C}_D\dot{\mathbf{u}}\cdot\hat{\eta} + \mathbf{K}\cdot\hat{\eta} = \mathbf{M}_b\mathbf{p}\cdot\hat{\eta}a_g \qquad \forall t \tag{15}$$

where the matrices $\mathbf{M}_b$, $\mathbf{K}_b$, $\mathbf{C}_F$ describe the mass, stiffness and damping of the frame and where $\mathbf{C}_D$ is the dissipative contribution of the dampers located at the tower base. This way, the tower influences only the damping operator and the shape of the virtual displacement field. Eqn. 15 can be rewritten as

$$\tilde{m}\ddot{\varphi} + (\tilde{c}_F + \tilde{c}_D)\dot{\varphi} + \tilde{k}\varphi = m^* a_g \tag{16}$$

where $\tilde{m} = \mathbf{M}_b\mathbf{L}\cdot\mathbf{L}$, $\tilde{c}_F = \mathbf{C}_F\mathbf{L}\cdot\mathbf{L}$, $\tilde{c}_D = \mathbf{C}_D\mathbf{L}\cdot\mathbf{L}$, $\tilde{k} = \mathbf{K}_b\mathbf{L}\cdot\mathbf{L}$, $m^* = \mathbf{M}_b\mathbf{p}\cdot\mathbf{L}$ are the scalar parameters describing the properties of the system reduced to a SDOF, and $\cdot$ denotes the scalar product. By solving Eqn. 15, the time-history of the base rotation is known, and the vector of nodal displacements of the MDOF system is determined by considering Eqn. (14).

3 CASE STUDY

3.1 Case study description

The application of the proposed approach is illustrated by considering a r.c. frame structure, with limited ductility, typical of many buildings designed during the 80s in Italy without any specific seismic detailing. Along the longitudinal direction, the structure consists of two external frames with 6 spans and a central one with 7 spans (Figure 2). The building has 5 storeys plus the roof.

The presented results concern three configurations, the bare existing frame (*As is*), the r,c, frame coupled with dissipative tower hinged at the foundation level and equipped with linear viscous dampers located at the base (*Retrofit*), and the r.c. frame coupled with an infinitely stiff dissipative tower (*Stiff*).

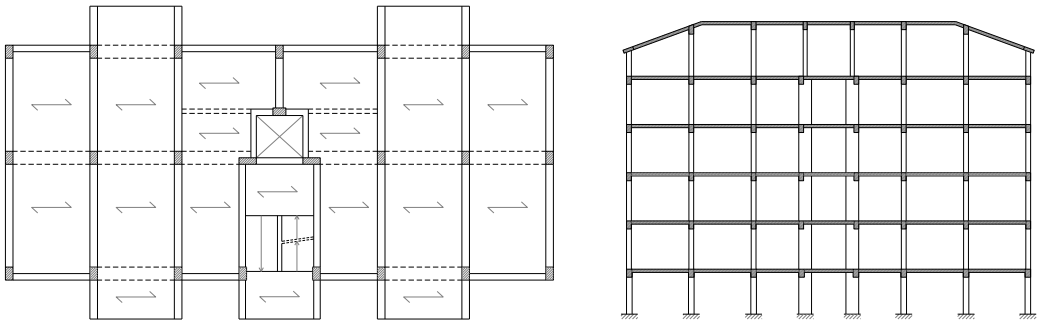

Figure 2: Planar view and longitudinal section of the bare building.

First, the previously described formulation is employed to investigate the influence of the external bracing properties on the overall dynamic properties of the coupled system, such as the modal displacement profile, the relevant internal action distribution and the modal damping ratios. Successively, the global effect of the retrofit on the seismic response is evaluated by solving the seismic problem with the modal decomposition method for the first two configurations (*As is* and *Retrofit*) and with a direct integration method for the last one (*Stiff*).

The dynamic system is described by considering only the motion along the longitudinal direction. The floors are assumed to be rigid in the horizontal plane and the masses are concentrated at the storey levels so that the vector of active degrees of freedom $\mathbf{x}$ collects the five storey motions only.

3.2 Modal properties of the undamped system

The bracing system influences both the stiffness and the damping properties of the coupled system, while its contribution to the masses is negligible. It is useful to separately analyze the variations on stiffness and damping and, for this purpose, the case of the added tower without dampers is considered separately from the case of the tower with dampers.

Table 1 reports, for the five modes of the bare building (*As is*), the vibration periods, the undamped natural frequencies and the participant mass ratios, defined as $M_i^* = (\mathbf{M}\mathbf{p} \cdot \boldsymbol{\psi}_i)^2 / \mathbf{M}\boldsymbol{\psi}_i \cdot \boldsymbol{\psi}_i$ where $\boldsymbol{\psi}_i$ are the eigenvectors of the undamped system.

T_i [s]	ω_0^2	M_i^*	ΣM_i^*
1.021	6.18	0.787	0.787
0.300	21.03	0.117	0.904
0.153	41.26	0.052	0.956
0.097	65.51	0.03	0.985
0.074	86.05	0.015	1

Table 1: Modal analysis results - *As is* configuration.

The modal analysis results of the coupled system in the *Retrofit* configuration are summarized in Table 2, where it can be observed that the first two vibration modes involve the 95% of the total mass and the second period reduces to about half the value obtained with the *As is* configuration. The third case, i.e. the existing frame coupled with an infinitely stiff tower (*Stiff*), is characterized by one vibration mode only (T=0.925 s) as it behaves like a SDOF system governed by the tower rocking motion.

T_i [s]	ω_0^2	M_i^*	ΣM_i^*
0.964	6.52	0.806	0.806
0.147	42.84	0.138	0.945
0.073	86.24	0.035	0.980
0.051	124.17	0.015	0.995
0.041	151.63	0.005	1

Table 2: Modal analysis results – *Retrofit* configuration.

Figure 3 reports and compares the values of the interstorey drifts along the building height corresponding to the first three modes of vibration for the *As is* and the *Retrofit* configurations. It can be observed that the addition of the towers yields a regularization of the drift demands along the building height, even though a higher value of the drift is required at the first level.

Figure 4 reports the distributions of the total shear forces in the *As is* and *Retrofit* cases for the first three modes, whereas Figure 5 shows, for the *Retrofit* configuration only, the storey shear demand for the building and the tower. It is worth to note that the shear contributions of the existing frame and the towers could have different signs at some levels and, for the considered case, the first mode shear forces acting on the existing frame is higher than the total shear force at the first level.

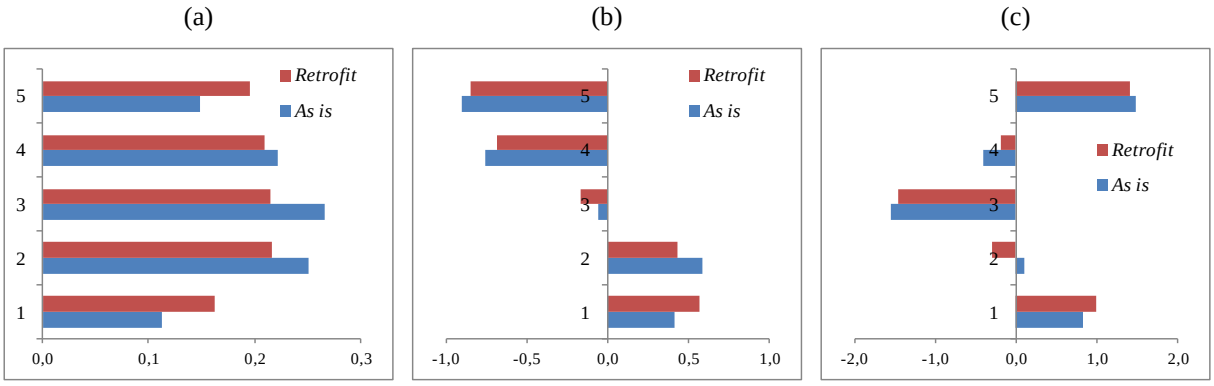

Figure 3: Interstorey drifts along the building height for mode 1 (a), mode 2 (b) and 3 (c).

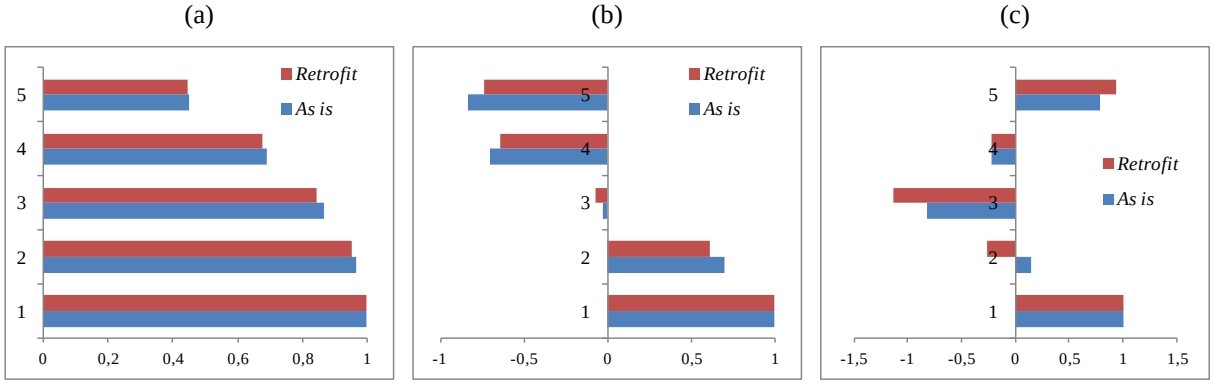

Figure 4: Total shear force comparison for mode 1 (a), mode 2 (b) and 3 (c).

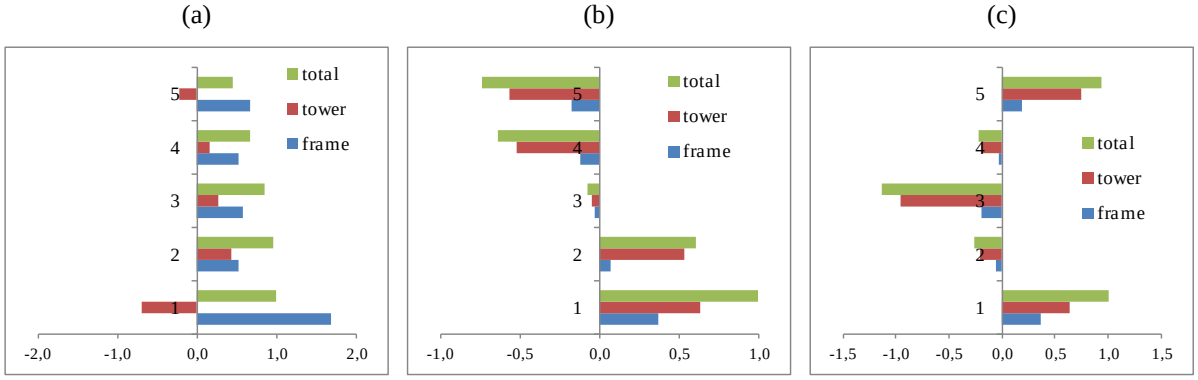

Figure 5: Shear force distribution for mode 1 (a), mode 2 (b) and 3 (c) – *Retrofit* configuration.

3.3 Modal properties of the damped system

The damping of the system is the sum of two contributions $\mathbf{C} = \mathbf{C}_F + \mathbf{C}_D$, the former is described by a Rayleigh damping matrix $\mathbf{C}_F = \alpha \mathbf{M} + \beta \mathbf{K}$, related to the existing frame, providing a inherent damping ξ=0.05 at the first two vibration modes. The latter contribution is due to the dampers and it is directly related to their displacements produced by the rocking motion.

A reference value of the damper dimensions is obtained by fixing a target total amount of the effective damping ratio β_{eff} =0.25 (0.05 due to the building and 0.20 due to the dampers), and by using the expression reported in ASCE/SEI 41-13 (2013)

$$\beta_{eff} = \beta + \frac{\sum_j W_j}{4\pi W_k} \tag{17}$$

where β is the damping in the structural frame (0.05), W_j the work done by j-th device in one complete vibration cycle and W_k is the maximum strain energy in the frame.

The retrofit configuration consists of two dampers placed as in Figure 1, whose viscous constant values are designed by employing eqn. (17) assuming that the system deforms according to its first undamped vibration mode. The total amount of added damping is measured by C_0=135020 kNs/m, which is the sum of the viscous damping constant of the two devices.

By means of the complex modal analysis it is possible to identify the damping ratio ξ_i corresponding to each one of the vibration modes, as shown in eqn. (9); moreover, by introducing a damper multiplier c for the total added damping C_0, it is possible to evaluate the variation of the modal properties at different damping levels, defined by the parameter c.

Figure 6(a) shows the influence of c on the vibration periods of the first three modes. The first three natural periods of the undamped system (dashed line in Figure 6) are 0.964 s the first period (blue line), 0.147 s the second (red line), and 0.073 s the third period (green line). The vibration periods of the coupled system decreases for increasing damping. For c=3.0, the first period attains the value 0.595 s, the second 0.141 s and the third 0.072 s. Thus, the amount of damping introduced influences significantly only the first vibration period of the system. Figure 6(b) shows the variation, with the total added damping c, of the damping ratio of the first, second and third vibration modes, ξ_1, ξ_2 and ξ_3. It also reports the variation of the estimate of the damping ratio β_{eff}, obtained by employing the approximate formula of Eqn.(17), for increasing values of c.

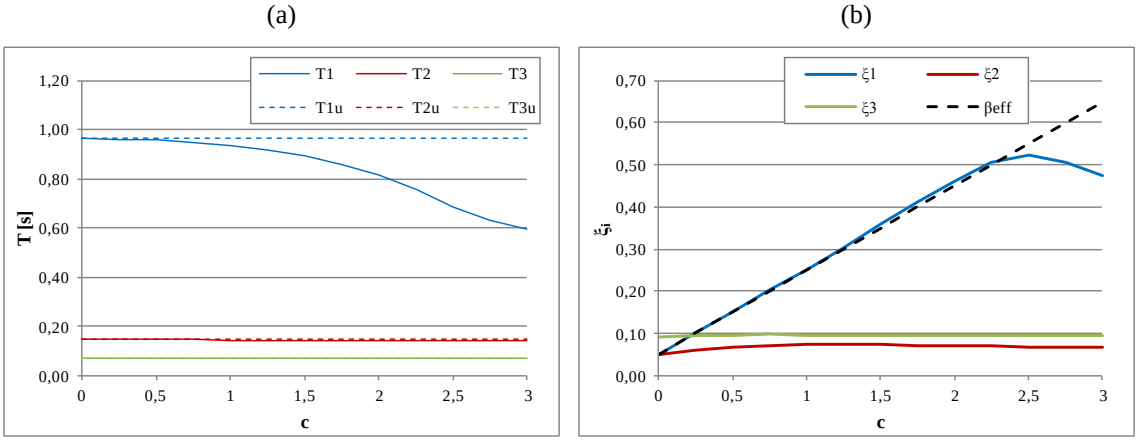

Figure 6: First three period trends (a) and first three modes damping trends (b) for increasing damping levels.

The first modal damping ratio ξ_1 is well approximated by the design formula of Eqn. (17) for ξ values up to 0.50 (c=2.25); for increasing values beyond this limit the amount of the effective damping decreases. As already observed for the periods, the influence of the damper dimensions on the second and third mode is negligible; the damping ratio varies in the range 0.050-0.067 with a maximum 0.074 when c=1.25 for the second mode, while for the third mode the range is 0.091-0.094 with a maximum value of 0.097 when c=0.75.

Due to the fact that all the dampers are concentrated at the tower base the system is notably non-classical damped and the extent of non-classical damping is synthetically quantified by the coupling index ρ (Claret e Venancio-Filho 1991), expressed as:

$$\rho = \max \left| \frac{\Xi_{ij}^2}{\Xi_{ii}\,\Xi_{jj}} \right| \quad (i,j=1,2,\ldots,m)\ i \neq j \tag{18}$$

where $\Xi_{ij} = \mathbf{C}_{xx}\boldsymbol{\psi}_i \cdot \boldsymbol{\psi}_j$ is the modal damping matrix component, $\mathbf{C}_{xx}$ and m are defined in section 2.1 and $\boldsymbol{\psi}_i$ are the eigenvectors of the undamped system. The index assumes the value 0 for classical damped systems and it spans the range [0,1] in the case of non-classical damping. Figure 7(a) shows the coupling index trend for increasing damping levels, while Figure 7(b) shows the values of ρ obtained for the damping target value c=1. In the latter case the maximum value of ρ is equal to 0.35 and corresponds to the coupling among the first and the second mode.

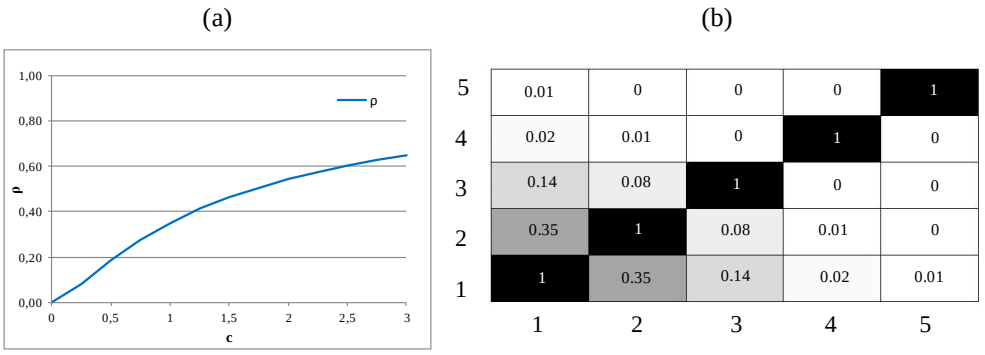

Figure 7: ρ-index: (a) trend for increasing damping levels; (b) values for the fifth modes of the system (c=1).

3.4 Seismic response

This section reports some results concerning the response of the three system configurations to a seismic input. The seismic action is determined by assuming the building located in Camerino (MC, Italy), with soil category C and topographical one T1, according to Italian code [20]. Seven artificial earthquakes, generated in accordance with Italian Standards, are considered. The results reported concern the most interesting parameters, i.e., the displacements, interstorey drifts, shear action distribution and the absolute accelerations; the values of these parameters reported below are the mean of the maximum values obtained for each of the seven time-histories analyses. The results related to the coupled systems (*Retrofit* and *Stiff* configurations) correspond to a total added damping multiplier c =1.

Table 3 reports the floor displacements and the interstorey drifts for the three configurations analyzed. The maximum top displacement, normalized with respect to that of the bare frame, is 54% for the *Retrofit* case and 58% for the *Stiff case*. Figure 8(a) and (b) show the distribution along the height of the building displacements x_i and interstorey drifts θ_i, for i=1,2,..,5. The reported values are normalized by dividing them by the corresponding values obtained at the 5th level in the *Stiff* configuration.

level	*As is*		*Retrofit*		*Stiff*	
	x_i [m]	θ_i [m]	x_i [m]	θ_i [m]	x_i [m]	θ_i [m]
1	0.013	0.013	0.008	0.008	0.009	0.009
2	0.040	0.028	0.019	0.011	0.018	0.009
3	0.068	0.029	0.029	0.011	0.027	0.009
4	0.092	0.026	0.040	0.011	0.036	0.009
5	0.109	0.019	0.050	0.010	0.046	0.009

Table 3: Floor displacements and drifts results

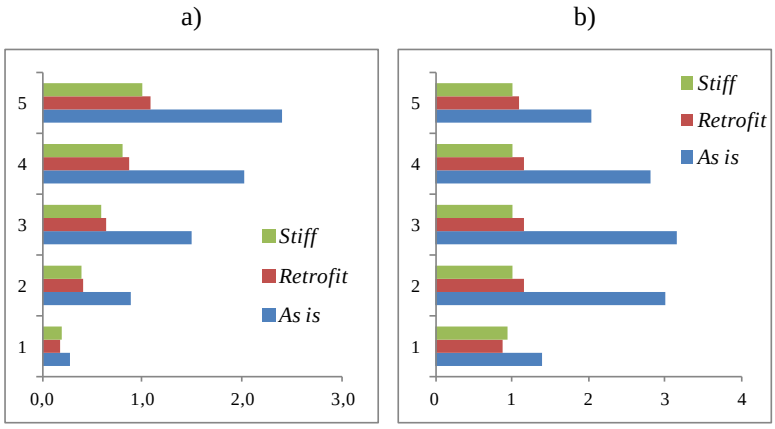

Figure 8: Displacements (a) and interstorey drifts (b) distributions for the three configurations.

It is noteworthy that the coupling with an infinitely stiff tower leads to a linear distribution of the displacements along the height. Moreover, the displacement demand at the first level is higher in the *Stiff* case than in the *Retrofit* case, while an opposite trend is observed at the top. This means that the regularization of the frame displacement distribution is achieved with the tower interacting with opposite forces at the base and at the top of the frame.

Having employed the complex mode superposition approach to solve the seismic problem, the contribution of the higher vibration modes to the response can be estimated by comparing the full response accounting for all the modes to the response obtained by considering the contribution of the first mode only. Table 4 reports the displacement response for the *As is* and the *Retrofit* case. Figure 9 comparises the displacement responses of the *As is* and *Retrofit* cases. In both the cases, the first mode contribution nearly controls the total response, while the effect of higher order modes is negligible.

level	*As is*		*Retrofit*	
	x_{full} [m]	x_1 [m]	x_{full} [m]	x_1 [m]
1	0.0129	0.0121	0.0080	0.0080
2	0.0405	0.0392	0.0188	0.0187
3	0.0684	0.0680	0.0295	0.0294
4	0.0918	0.0920	0.0399	0.0399
5	0.1092	0.1081	0.0497	0.0496

Table 4: Floor displacements and drifts results.

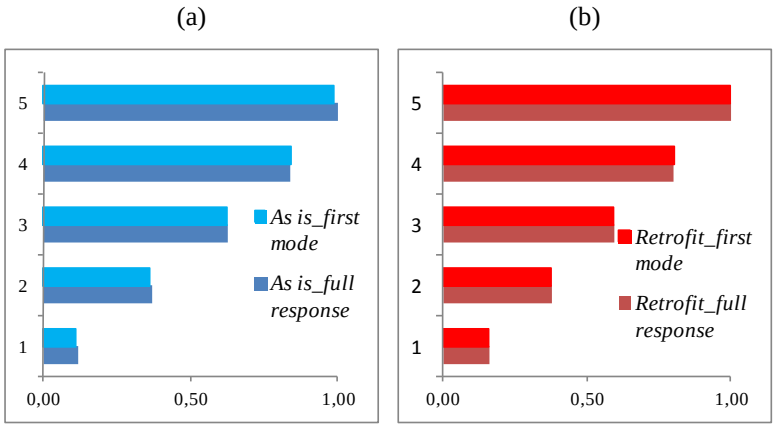

Figure 9: Contribution of the first mode to the full response of the (a) *As is* and (b) *Retrofit* cases.

Table 5 reports the shear actions resisted by the frame in the three configurations; for the *Retrofit* case the shear actions resisted by the tower and the total shear actions are also reported. It is noteworthy that the maximum shear for the tower and the frame may not occur at the same instant of time for all the records considered. As already discussed for the displacements, also the global shear demand decreases, but in a less significant way. The relative reduction of the maximum base shear acting on the frame, with respect to the bare frame, is nearly 19% for the *Retrofit* case and 6% for the *Stiff* one.

Figure 10(a) shows the shear actions distribution along the height of the frame, normalized after dividing them by the value of the base shear in the *Retrofit* configuration. Figure 10(b) shows the shear forces in the frame and the tower for the *Retrofit* case; the values are normalized with respect to the total base shear, obtained as the sum of the building plus the tower one.

level	*As is*	*Retrofit*			*Stiff*
	$V_{i,\text{frame}}$ [kN]	$V_{i,\text{frame}}$ [kN]	$V_{i,\text{tower}}$ [kN]	$V_{i,\text{total}}$ [kN]	$V_{i,\text{frame}}$ [kN]
1	5215.67	4232.33	2661.26	3544.64	4877.47
2	4789.76	1348.32	1915.45	3060.02	831.69
3	4197.01	1455.88	1292.91	2543.55	1290.06
4	3686.99	1366.94	1169.54	2336.51	1095.12
5	2755.01	1740.77	1020.58	1819.51	1643.12

Table 5: Shear actions results.

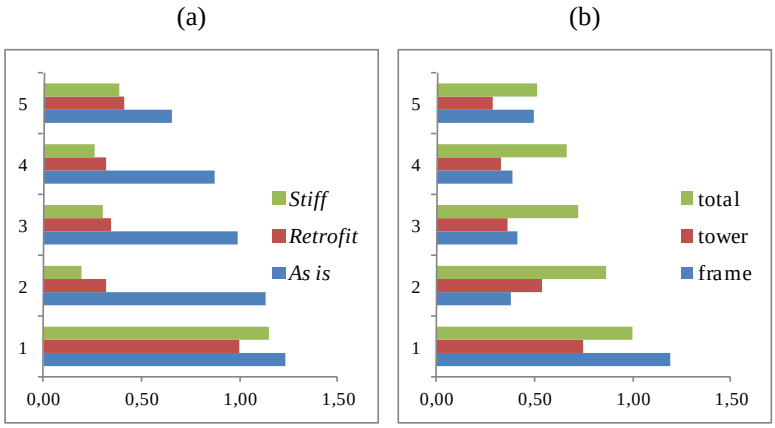

Figure 10: (a) Shear actions resisted by the frame in the three configurations and (b) shear actions resisted by the tower, the building and the frame compared to the total shear in the *Retrofit* case.

The complex mode superposition is also employed to estimate the contribution of the higher order modes of vibration on the shear actions before and after the retrofit. Table 6 reports the shear actions distribution resisted by the frame in the *As is* case and the contributions of both the frame and the tower in the *Retrofit* one, due to the full response and the first mode. Differently from the case of the displacements, the contribution of higher order modes is important as the values of both the total shear response and the tower shear response are higher than the corresponding values obtained by considering the first mode only. However, the building response appears to be still dominated by the first mode of the coupled system. These observations, together with the fact that the increase of damping ratio after the retrofit is lower for the higher modes than for the first mode, could explain why the reduction of the displacement demand is higher than that of the base shear.

level	*As is*		*Retrofit*					
	V_{full} [kN]	V_1 [kN]	$V_{\text{frame\_full}}$ [kN]	V_{frame1} [kN]	$V_{\text{tower\_full}}$ [kN]	V_{tower1} [kN]	$V_{\text{total\_full}}$ [kN]	V_{total1} [kN]
1	5215.7	4751.3	4232.3	4202.4	2661.3	2204.3	3544.6	2963.0
2	4789.8	4600.0	1348.3	1329.6	1915.4	1734.4	3060.0	2825.4
3	4197.0	4116.0	1455.9	1440.3	1292.9	1344.5	2543.5	2507.4
4	3687.0	3276.9	1366.9	1316.7	1169.5	958.4	2336.5	2007.0
5	2755.0	2142.6	1740.8	1665.6	1020.6	687.9	1819.5	1328.4

Table 6: Higher order modes influence on the shear actions.

Figure 11(a) depicts the first mode contribution to the full shear response of the frame in the *As is* case, normalized by the value of the total base shear. Figure 11(b) shows the same comparison for the *Retrofit* configuration. Figure 12 a) and b) depicts the first mode contribution to the full shear response of the tower and of total system for the *Retrofit* case.

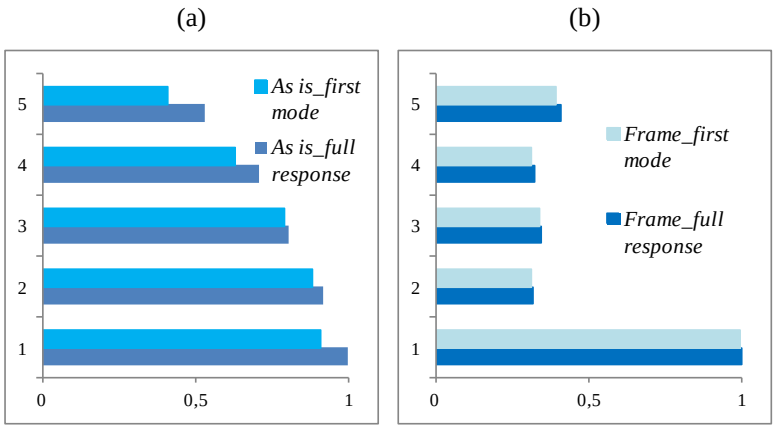

Figure 11: First mode contribution on the total shear response of the frame in the (a) *As is* case and (b) *Retrofit* configuration.

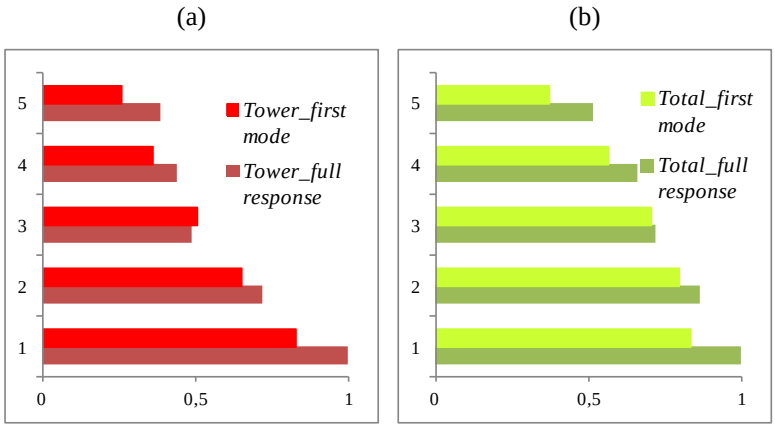

Figure 12: First mode contribution in the *Retrofit* case (a) on the total shear response of the tower and (b) on the overall response.

Table 7 contains the absolute acceleration values observed at the various levels of the building for the configurations investigated..

level	*As is* $\ddot{x}_i$ [m/s^2]	*Retrofit* $\ddot{x}_i$ [m/s^2]	*Stiff* $\ddot{x}_i$ [m/s^2]
1	2.98	2.77	2.10
2	3.86	3.36	1.80
3	4.58	3.02	1.70
4	4.14	2.34	1.97
5	5.27	3.49	2.69

Table 7: Absolute accelerations.

The coupling of the building with the external dissipative system induces a relative reduction of the maximum absolute acceleration values with respect to the values observed in the *As is* case. This result is noteworthy especially for all the non structural elements (e.g. medical devices) that could be hosted in a structure. Figure 13 shows the values of the absolute acceleration distribution along the height of the normalized by the value at the 5th floor observed for the *Stiff* case. The relative reduction of acceleration is nearly 34% for the *Retrofit* case and 48% for the *Stiff* case

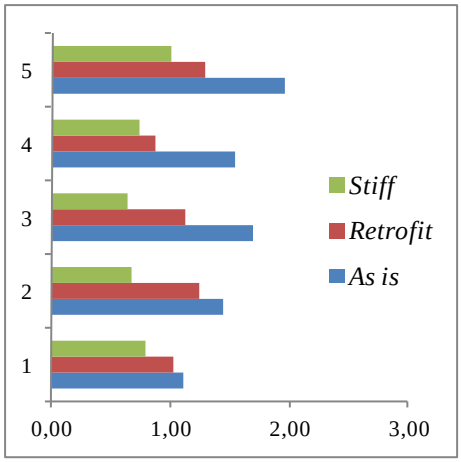

Figure 13: Absolute acceleration distribution along the height.

4 CONCLUSIONS AND FURTHER STUDIES

This paper presents and analyzes three alternative categories of external viscous dampers retrofitting system which exhibit a different kinematic behavior. Among them, the dissipative tower configuration is deeply investigated, in terms of modal properties and seismic response of the coupled system.

A problem formulation concerning the dynamic behavior of the coupled system is presented in general terms. The results include also two limit configurations, the bare building and the coupling with an infinitely stiff dissipative tower.

The case study results reveal that the addition of the towers leads to a regularization of the drift demand along the building height. After the retrofit, the shear force distribution in the existing frame could significantly change and the system is notably non-classical damped due to the fact that all the dampers are concentrated at the base of the tower. Moreover, from the dynamic response it appears that higher order vibration modes have a notable influence on the internal actions demand, while are almost negligible for the displacement response.

The *Stiff* configuration highlights the benefits and drawbacks of the dissipative system. This limit configuration provides the best distribution of the inter-storey drifts but provides high shear forces in the frame, which are larger than the forces observed in the *Retrofit* case and similar to the forces observed in the *As is* case.

A deeper and wider investigation is still necessary for a full comprehension of the problem, and should be oriented to understand the optimal stiffness range of the dissipative tower.

REFERENCES

[1] T.T. Soong, G.F. Dargush, *Passive Energy Dissipation Systems in Structural Engineering*. Wiley: New York, 1997.

[2] T.T. Soong, B.F. Spencer ,Supplemental energy dissipation: state-of-the art and state-of-the practice. *Engineering Structure*, **24**, 243–259, 2002.

[3] C. Christopoulos, A. Filiatrault, *Principles of Passive Supplemental Damping and Seismic Isolation*. IUSS Press: Pavia, Italy 2006.

[4] L. Ragni, L. Dezi, A. Dall'Asta, G. Leoni, HDR devices for the seismic protection of frame structures: Experimental results and numerical simulation. *Earthquake Engineering and Structural Dynamics*, DOI:10.1002/eqe891Vol. **38**(10), 1199-1217 (ISSN: 0098-8847, eISSN: 1096-9845), 2009.

[5] J.K. Whittle, , M.S. Williams, , T.L. Karavasilis, , A. Blakeborough, ,. Comparison of Viscous Damper Placement Methods for Improving Seismic Building Design. *Journal of Earthquake Engineering*, **16**(4), 540-560, 2012.

[6] J.S. Hwang, W.C. Lin, N.J. Wu, Comparison of distribution methods for viscous damping coefficients to buildings. *Structure and Infrastructure Engineering: Maintenance, Management, Life-Cycle Design and Performance*, **9**(1):28-41, 2013.

[7] O. Lavan , M. Avishur, . Seismic behaviour of viscously damped yielding frames under structural and damping uncertainties. *Bulletin of Earthquake Engineering*, **11**(6), 2309-2332, 2013.

[8] E. Tubaldi, L. Ragni, A. Dall'Asta, Probabilistic seismic response assessment of linear systems equipped with nonlinear viscous dampers. *Earthquake Engineering and Structural Dynamics*, DOI: 10.1002/eqe.2462, 2014.

[9] E. Tubaldi, M. Barbato, A. Dall'Asta, Efficient approach for the reliability-based design of linear damping devices for seismic protection of buildings. *ASCE-ASME Journal of Risk and Uncertainty if Engineering Systems, Part A: Civil Engineering, special issue on Stochastic Dynamics and Reliability Analysis of Structural and Mechanical Systems Subject to Environmental Excitations*. DOI: 10.1061/AJRUA6.0000858, 2015.

[10] A. Dall'Asta, E. Tubaldi, L. Ragni, Influence of the nonlinear behaviour of viscous dampers on the seismic demand hazard of building frames. *Earthquake Engineering and Structural Dynamics*, **45**(1), 149-169, 2016.

[11] F. Freddi, E. Tubaldi, L. Ragni, A. Dall'Asta, 2012. Probabilistic performance assessment of low-ductility reinforced concrete frames retrofitted with dissipative braces. *Earthquake Engineering and Structural Dynamics*, **42(7)**, 993-1011.

[12] T. Trombetti, , S. Silvestri, , Novel Schemes for Inserting Seismic Dampers in Shear-Type Systems Based Upon the Mass Proportional Component of the Rayleigh Damping Matrix. *Journal of Sounds and Vibrations*, **302**, 486-526, 2007.

[13] V. Gattulli, , F. Potenza, , M. Lepidi, Damping performance of two simple oscillators coupled by a dissipative connection. *Journal of Sound and Vibration*, **332**(26), 6934-6948, 2013.

[14] E. Tubaldi, M.Barbato, A. Dall'Asta, , Performance-based seismic risk assessment for buildings equipped with linear and nonlinear viscous dampers. *Engineering Structures*, **78**, 90-99, 2014.

[15] E. Tubaldi, Dynamic behavior of adjacent buildings connected by linear viscous/viscoelastic dampers. *Structural Control and Health Monitoring*, **22**(8), 1086-1102, 2015.

[16] C. Passoni, A. Belleri, A. Marini, P. Riva, Existing structures connected with dampers: state of the art and future developments, *2nd European Conference on Earthquake Engineering and Seismology*, Istanbul, Turkey, August 25-29, 2014,.

[17] D. Roia, F. Gara, A. Balducci, L.Dezi, , Dynamic tests on an existing r.c. school building retrofitted with "dissipative towers", *11th International Conference on Vibration Problems*, Lisbon, Portugal, September 9-12, 2013.

[18] D. Roia, F. Gara, A. Balducci, , L. Dezi, , Ambient vibration tests on a reinforced concrete school building before and after retrofitting works with external steel" dissipative towers", *Proceedings of the 9th International Conference on Structural Dynamics, EURODYN 2014*, Porto, Portugal, June 30-July 2, , 2014.

[19] A. Balducci, Dissipative Towers. Application n. EP2010074723820100831, WO2010EP62748 20100831, International and European classification E04H9/02 – Italian concession n 0001395591, 2005.

[20] Nuove Norme Tecniche per le Costruzioni, D.M. Infrastrutture 14 gennaio 2008, Circolare 02 febbraio 2009 n. 617/C.S.LL.PP. 2009 (in Italian).